Synthesis and Characterization of an Al_{69}^{3-} Cluster with 51 Naked Al Atoms: Analogies and Differences to the Previously Characterized Al_{77}^{2-} Cluster

H. Köhnlein, A. Purath, C. Klemp, E. Baum, I. Krossing, G. Stösser, and H. Schnöckel*

Institut für Anorganische Chemie, Universität Karlsruhe (TH), Engesserstrasse, Geb. 30.45 D-76128 Karlsruhe, Germany

Received April 24, 2001

A disproportionation process of a metastable AlCl solution with a simultaneous ligand exchange—Cl is substituted by $N(SiMe_3)_2$—leads to a $[Al_{69}\{N(SiMe_3)_2\}_{18}]^{3-}$ cluster compound that can be regarded as an intermediate on the way to bulk metal formation. The cluster was characterized by an X-ray crystal structural analysis. Regarding its structure and the packing within the crystal, this *metalloid* cluster with 4 times more Al atoms than ligands is compared to the $[Al_{77}N(SiMe_3)_2\}_{20}]^{2-}$ cluster that has been published four years ago. Although there is a similar packing density of the Al atoms in both clusters as well as in Al metal, the X-ray structural analysis shows significant differences in topology and distance proportions. The differences between these—at a first glance almost identical—Al clusters demonstrate that results of physical measuring, e.g., of nanostructured surfaces which carry supposedly identical cluster species, have to be interpreted with great caution.

Introduction

Since many years subhalides of the 13th group elements boron, indium, and thallium have been well-established. In the case of indium and thallium, these subhalides can be synthesized without problems.[1] Already 50 years ago, molecular aluminum monohalides were successfully characterized at high temperatures in the gas phase.[2] About 30 years ago, they were characterized as monomers and dimers in matrix experiments,[3] and only in the past decade they were synthesized on a preparative scale.[4] The reason for this late development is—among other problems—the instability of the Al^I and Ga^I halides toward disproportionation. Gaseous MX high-temperature molecules (M = Al, Ga; X = Cl, Br, I) which can be synthesized, e.g., by passing HX gas over the liquid metal at temperatures near 1000 °C and at pressures of about 10^{-3} mbar, are thermodynamically stable only under these conditions. Keeping these problems in mind, our group applied the co-condensation technique[5] in order to synthesize AlX species in gram-scales.[6] To avoid disproportionation when only slowly cooling, the MX species are quenched immediately after their formation on a surface which is cooled by liquid nitrogen together with a suitable donor-containing solvent mixture, e.g. toluene with THF, NEt_3 or Et_2O. Upon thawing of the solvent matrix, the co-condensate is collected in a flask and can be stored at −80 °C for a few months. The thermodynamically favored disproportionation of aluminum(I), respectively gallium(I) halides to the metal and the trihalide can be kinetically controlled by varying either the halide, the donor or the temperature. The thus obtained metastable Al^I and Ga^I halide solutions showed to be ideal precursors for the synthesis of interesting subvalent Al and Ga compounds: intermediates (on the way to metal formation) with newly tied M−M bonds can be stabilized by metathesis reactions replacing the halide by a bulky fragment. Whereas *metalloid*[7] Ga clusters were synthesized by a reaction of gallium(I) halide solutions with different ligands, e.g., $Si(SiMe_3)_3$(*Hypersilyl*),[8] $C(SiMe_3)_3$(*Trisilyl*),[9] or $N(SiMe_3)_2$,[10] the latter substituent seems to be especially suited to stabilize

* To whom correspondence should be sent. Fax: (+49)721-608-4854. E-mail: Hansgeorg.Schnoeckel@chemie.uni-karlsruhe.de.

(1) Morrison, J. A. *Chem. Rev.* **1991**, *91*, 35.
(2) (a) Klemm, H.; Voss, E.; Geiersberger, K. *Z. Anorg. Allg. Chem.* **1948**, *256*, 15, 24. (b) Huber, P.; Herzberg, G. *Molecular Structure IV, Constants of Diatomic Molecules*; Van Nostrand, Reinhold: New York, 1979; pp 18−22, 26.
(3) (a) Schnöckel, H. *Z. Anorg. Allg. Chem.* **1976**, *424*, 203. (b) Schnöckel, H. *J. Mol. Struct.* **1978**, *50*, 267.
(4) (a) Tacke, M.; Schnöckel, H. *Inorg. Chem.* **1989**, *28*, 2895. (b) $Al_4Br_4 \cdot 4NEt_3$: Mocker, M.; Robl, C.; Schnöckel, H. *Angew. Chem., Int. Ed. Engl.* **1994**, *106*, 1860; *33*, 1754. (c) $Al_4I_4 \cdot 4D$: Ecker, A.; Schnöckel, H. *Z. Anorg. Allg. Chem.* **1998**, *624*, 813. (d) $Ga_8I_8 \cdot 6NEt_3$: Doriat, C.; Friesen, M.; Baum, E.; Ecker, A.; Schnöckel, H. *Angew. Chem., Int. Ed. Engl.* **1997**, *109*, 2057; *36*, 1969.
(5) Timms, P. L. *Adv. Inorg. Chem. Radiochem.* **1972**, *14*, 142.
(6) Dohmeier, C.; Loos, D.; Schnöckel, H. *Angew. Chem., Int. Ed. Engl.* **1996**, *108*, 141; *35*, 129.
(7) In 1966, F. A. Cotton defined *clusters of metal atoms* as molecules, where two or more metal atoms—apart from being bonded to other nonmetal atoms—are also bonded to each other. This description applies to numerous compounds with different bonding relations as $Fe_2(CO)_9$, $[Au_{39}(PPh_3)_{14}C_6]^{2+}$, $[HNi_{38}(CO)_{42}Cl_6]^{5-}$, or $Pd_{145}(CO)_x(PEt_3)_{30}$. For clusters such as the aforementioned Al_mR_n species (with $m > n$), whose common characteristic is that the number of direct metal−metal interactions is larger than the number of metal−ligand interactions (2e2c), we introduced the new term *metalloid* (metal-like) cluster to draw a more distinct boundary to Cotton's *metal atom clusters*. References: (a) *Metal atom clusters*: Cotton, F. A. *Q. Rev. Chem. Soc.* **1966**, 389. (b) *Metalloid clusters*: Schnepf, A.; Stösser, G.; Schnöckel, H. *J. Am. Chem. Soc* **2000**, *122*, 9178. Ref 11b. (c) $Fe_2(CO)_9$: Cotton, F. A.; Troup, J. M. *J. Chem. Soc., Dalton Trans.* **1974**, 800. (d) $[Au_{39}(PPh_3)_{14}C_6]^{2+}$: Teo, B. K.; Shi, X.; Zhang, H. *J. Am. Chem. Soc.* **1992**, *114*, 2743. (e) $[HNi_{38}(CO)_{42}Cl_6]^{5-}$: Ceriotti, A.; Fait, A.; Longoni, G.; Piro, G. *J. Am. Chem. Soc.* **1986**, *108*, 8091. (f) $Pd_{145}(CO)_{60}(PEt_3)_{30}$: Tran, N. T.; Powell, D. R.; Dahl, L. F. *Angew. Chem., Int. Ed.* **2000**, *112*, 4287; *39*, 4121.
(8) (a) $Ga_{22}[Si(SiMe_3)_3]_8$: Schnepf, A.; Weckert, E.; Linti, G.; Schnöckel, H. *Angew. Chem., Int. Ed.* **1999**, *111*, 3578; *38*, 3381. (b) $[Ga_{26}\{Si(SiMe_3)_3\}_9][Li(THF)_4]_2$: Rodig, A.; Linti, G. *Angew. Chem., Int. Ed.* **2000**, *112*, 3076; *39*, 2952. (c) $[Ga_9\{Si(SiMe_3)_3\}_6][Li(THF)_4]$: Köstler, W.; Linti, G. *Angew. Chem., Int. Ed. Engl.* **1997**, *109*, 2758; *36*, 2644.
(9) (a) $Ga_4[C(SiMe_3)_3]_4$: Uhl, W.; Hiller, W.; Layh, M.; Schwarz, W. *Angew. Chem., Int. Ed. Engl.* **1992**, *104*, 1378; *31*, 1364. (b) $Ga_8[C(SiMe_3)_3]_6$: Schnepf, A.; Köppe, R.; Schnöckel, H. *Angew. Chem., Int. Ed.* **2001**, *113*, 1287; *40*, 1251.
(10) $[Ga_{84}\{N(SiMe_3)_2\}_{20}]^{4-}$: Schnepf, A.; Schnöckel, H. *Angew. Chem.* **2001**, *113*, 734; *Angew. Chem., Int. Ed. Engl.* **2001**, *40*, 712.

10.1021/ic0104297 CCC: $20.00
Published on Web 07/17/2001

the respective Al compounds: Thus, $LiN(SiMe_3)_2$ reacts with ether-stabilized AlI solution to the $Al_{77}R_{20}^{2-}$ [R = $LiN(SiMe_3)_2$] cluster and to the partly substituted $Al_{14}I_6R_6^{2-}$ cluster; with AlCl solution the $Al_7R_6^-$ cluster and the $Al_{12}R_8^-$ cluster were synthesized as intermediates[11] on the way to aluminum metal.

Experimental Section

Preparation of $LiN(SiMe_3)_2$. Donor-free lithium−bis(trimethylsilyl)-amide was synthesized by metalation of bis(trimethylsilyl)amine with a solution of *n*-butyllithium in pentane.[12] The product was recrystallized several times from pentane. ^{1}H NMR (C_6D_6) 0.13 ppm, ^{7}Li NMR (C_6D_6) 0.89 ppm, ^{13}C NMR (C_6D_6) 5.85 ppm, ^{29}Si NMR (C_6D_6) −10.0 ppm.

Synthesis of 1a. A total of 40 mmol gaseous AlCl were co-condensed with 60 mL toluene and 20 mL diethyl ether at −196 °C. Next, 9.5 mL of the ca. 0.29 molar (2.75 mmol) dark reddish-brown $AlCl{\cdot}Et_2O$ solution was added to 500 mg (3.00 mmol) donor free $LiN(SiMe_3)_2$ at 25 °C. After 1 h the amide dissolved and LiI precipitated, which was then filtered. For 1.5 h the solution was heated to 60 °C. Apart from the precipitation of elemental aluminum we obtained **1a** as dark reddish-brown sticks which chemically and mechanically proved to be extremely instable. Yield of crystalline solid material: 5% (8 mg, 0.0014 mmol).

Synthesis of 1b. A solution of AlCl (10 mL, 2.90 mmol) in toluene/Et_2O (3:1) (cf. **1a**) was added to 485 mg (2.90 mmol) $LiN(SiMe_3)_2$ at −78 °C. The reacting solution was warmed to room temperature within 1 day. After 1 h of heating at 60 °C LiCl precipitated which was subsequently filtered. After storage at +60 °C for 2 months, elemental aluminum as well as **1b** which appeared as dark reddish-brown cubes crystallized from the solution. Yield of crystalline solid material: 7% (10 mg, 0.0020 mmol).

X-ray Crystallography. The data set of **1a** was collected using a NONIUS KAPPA CCD diffractometer with graphite-monochromated Mo Kα radiation (λ = 0.71073 Å) at 200 K.[13] In the case of the species **1b** we used a STOE IPDS diffractometer with the same X-ray source. The structures were solved by direct methods (Shelxs 97). A total of 1092 and 2098 parameters for **1a** and **1b**, respectively, were refined by full matrix least squares against F^2 (Shelxl 97) with anisotropic thermal parameters for all non-hydrogen atoms. H atoms were refined on calculated positions according to the riding model.

Table 1. Crystallographic Data for **1a**

chemical formula: $C_{120}H_{372}Al_{69}Li_3N_{18}O_{12}Si_{36}$	formula weight: 5482.34 g mol^{-1},
a = 29.1720(6) Å	space group: $C\,2/c$ (no. 7)
b = 37.6650(8) Å	T = −100 °C
c = 31.5020(6) Å	λ = 0.71073 Å
β = 96.107(3)°	D_{calc} = 1.064 g cm^{-3}
V = 34416 (12) Å^3	μ = 3.40 cm^{-1}
Z = 4	R^a = 0.1296
	$R_w{}^b$ = 0.4275

^{a} $R = (\sum \mid |F_o| - |F_c| \mid)/(\sum |F_o|)$. ^{b} $R_w = [(\sum w(F_o^2 - F_c^2)^2)]^{1/2}$; $w = 1/(\sigma^2(F_o^2) + (0.115)P^2 + 0.4631P)$.

Table 2. Crystallographic Data for **1b**

chemical formula: $C_{117}H_{333}Al_{69}Li_{1.5}N_{18}O_5Si_{36}$	formula weight: 4956.28 g mol^{-1}
a = 28.6252(18) Å	space group: $P\,2_1/c$ (no. 14)
b = 28.4753(13) Å	T = −73 °C
c = 43.5454(24) Å	λ = 0.71073 Å
β = 107.328(7)°	D_{calc} = 0.972 g cm^{-3},
V = 33883(4) Å^3	μ = 3.40 cm^{-1}
Z = 4	R^a = 0.1152
	$R_w{}^b$ = 0.2907

^{a} $R = (\sum \mid |F_o| - |F_c| \mid)/(\sum |F_o|)$. ^{b} $R_w = [(\sum w(F_o^2 - F_c^2)^2)]^{1/2}$; $w = 1/(\sigma^2(F_o^2) + (0.115)P^2 + 0.4631P)$.

Results

Here we discuss a remarkable *metalloid* aluminum cluster anion, $[Al_{69}\{N(SiMe_3)_2\}_{18}]^{3-}$ (**1**), which could be isolated and structurally characterized as an intermediate stage of the disproportionation of Al^I compounds to aluminum metal and Al^{III} compounds. The synthesis of **1** succeeded using $AlCl{\cdot}OEt_2$ solution and LiR [R = $N(SiMe_3)_2$] under similar reaction conditions applied for the synthesis of the Al_{77} cluster starting from $AlI{\cdot}OEt_2$ and LiR. A conceivable total reaction for the Al_{69} cluster synthesis is formulated in eq 1:

$$96\ \overset{+1}{Al}Cl{\cdot}Et_2O + 18\ LiR \rightarrow [\overset{+0.217}{Al}_{69}R_{18}]^{3-}[Li(OEt_2)_4]_3^+ + 27\ \overset{+3}{Al}Cl_3{\cdot}Et_2O + 15\ LiCl{\cdot}3Et_2O + 12\ Et_2O \quad (1)$$

From different runs of the reaction two species of **1** could be isolated. The X-ray structural analysis of the black crystalline products showed the compounds to be $[Al_{69}\{N(SiMe_3)_2\}_{18}][Li(OEt_2)_4]_3{\cdot}6$ toluene (**1a**) and $[Al_{69}\{N(SiMe_3)_2\}_{18}][Li(OEt_2)_3]_2[Li(OEt_2)_4]{\cdot}n$ toluene (**1b**).[14] The cluster anion which is structurally identical in **1a** and **1b**[15] is shown in Figure 1a.

In Figure 1b the corresponding Al−Al bonds between the Al shells as well as the $N(SiMe_3)_2$ groups have been omitted for a better visualization of the shell-like structure.

At first glance, the structure of the cluster compound $[Al_{77}\{N(SiMe_3)_2\}_{20}][Li_2I(OEt_2)_5]_2{\cdot}2$ toluene (**2**; Figure 2), which was synthesized in our group in 1996, seems to strongly resemble to **1**.

A common characteristic of both nanosized clusters **1** and **2** is the metal frame of three shells, the outer shell consisting of AlR units. The diameter of the Al_{69} unit amounts to 1.27 nm, that of the Al_{77} to 1.30 nm. Considering this aspect in the empirical formula, **1** can be regarded as $[Al_{51}(AlR)_{18}]^{3-}$ and **2** as $[Al_{57}(AlR)_{20}]^{2-}$. Due to the different number of metal atoms—however a similar Al/R ratio (**1**: 3.83, **2**: 3.85) is observed—the geometries of the cluster frames differ already in the inner shell.

Comparison of the Al Shells for 1 and 2. In **1** and **2** the central Al atom is surrounded by 12 Al atoms, which for their part are also coordinated by 9 atoms (cf. Tables 3 and 4). The decahedral shell of **1** (Figure 1a) exhibits a distorted D_{5h} symmetry, with the five-membered rings not being in exactly eclipsed position to each other and also having different edge lengths (distances from 2.717 to 3.232 Å). The coordina-

(11) (a) $Al_{77}R_{20}^{2-}$: Ecker, A.; Weckert, E.; Schnöckel, H. *Nature* **1997**, *387*, 379. (b) $Al_{14}I_6R_6^{2-}$: Köhnlein, H.; Stösser, G.; Baum, E.; Möllhausen, E.; Huniar, U.; Schnöckel, H. *Angew. Chem.* **2000**, *112*, 828; *Angew. Chem., Int. Ed.* **2000**, *39*, 799. (c) $Al_7R_6^-$: Purath, A.; Köppe, R.; Schnöckel, H. *Angew. Chem., Int. Ed.* **1999**, *111*, 3114; *38*, 2926; (d) $Al_{12}R_8^-$: Purath, A.; Schnöckel, H. *Chem. Commun.* **1999**, 1933.

(12) Wannagat, U.; Niederprüm, H. *Chem. Ber.* **1961**, *94*, 1540.

(13) Since the single crystals of **1a** are extremely sensitive to air and moisture the measuring was performed by the group of R. Minkwitz, University of Dortmund. Their special technique for the cooled transfer of sensitive crystals from the reaction flask to the diffraction goniometer head enabled successful crystal mounting.

(14) According to the X-ray structural analysis **1a** and **1b** differ in the number of toluene molecules and Li^+cations: In **1b** only 1.5 toluene molecules and 1.5 of three cations could be properly detected. To elucidate the charge of the anion the compounds were investigated by ESR spectroscopy. The lack of any signal indicates the total number of electrons within the cluster anion to be even. Since a neutral $Al_{69}R_{18}$ cluster would have an odd electron number the stoichiometry of the species **1a** with three $[Li(OEt_2)_4]^+$ cations per cluster anion is consistent with the result of the ESR experiment. Considering the fact that **1a** and **1b** both possess structurally identical cluster anions, we conclude that in both compounds an anion-to-cation ratio of 1:3 was realized. Obviously the remaining 1.5 cations in **1b** are "smeared" over the remaining gaps.

(15) Therefore we will not distinguish between both species in the following, except for observations made concerning the packing of ions.

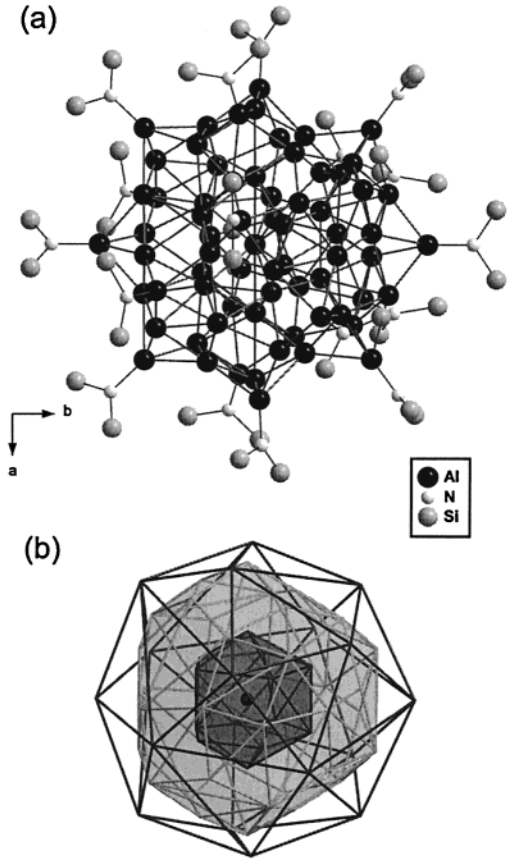

Figure 1. (a) Molecular structure of the anion of **1** (methyl groups excluded). (b) Shell-like Al frame of **1** (from central atom to the exterior): 1st shell, 12 Al atoms; 2nd shell, 38 Al atoms; 3rd shell, 18 Al atoms.

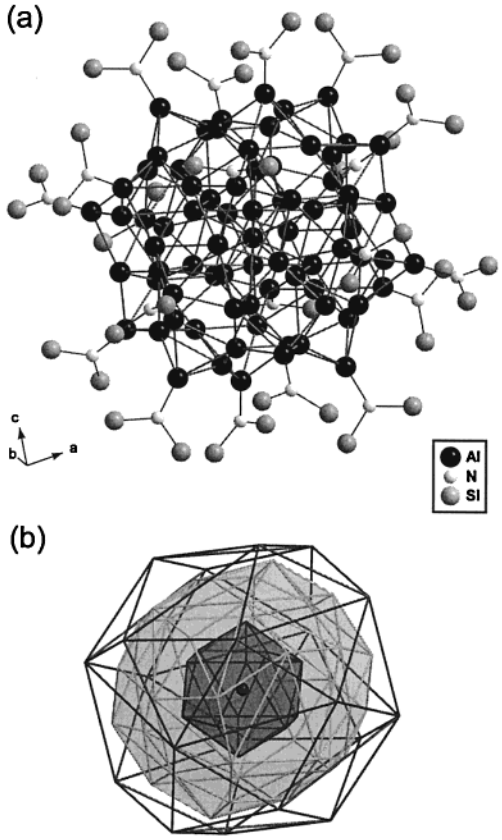

Figure 2. (a) Molecular structure of the anion of **2** (methyl groups excluded). (b) Shell-like Al skeleton of **2** (from central atom to exterior): 1st shell, 12 Al atoms; 2nd shell, 44 Al atoms; 3rd shell, 20 Al atoms.

Table 3. Al−Al Distances within and between (e.g., 1 → 2) the Al_{69} Cluster Shells

shell	center	1	1 → 2	2	2 → 3	3
atoms	1	12		38		18
c.n.[a]	12	9[b]	4	7[c]	2	(4)[d]
$d_{\text{minimal (Å)}}$	2.681	2.708	2.650	2.607	2.543	(4.663)
$d_{\text{maximal (Å)}}$	2.894	2.991	2.942	2.968	2.883	(5.700)
$d_{\text{average (Å)}}$	2.783	2.782	2.783	2.797	2.683	(5.103)

[a] c.n. = coordination number. Number of the next atoms surrounding the central atom and forming the 1st shell ("Center"; column 2), coordination of each of the atoms in the 1st shell by the atoms in the 2nd shell ("1 → 2"; column 4) etc. For the coordination within the 1st and 2nd shell (column 3 and 5, respectively) a total c.n. is given. All numbers represent average values (except for column 2). [b] The total c.n. of an atom in the 1st and 2nd shell is the sum of the next atoms within the same shell and the next atoms of the neighboring shells. Total c.n. = $\text{c.n.}_{1\text{·shell}\rightarrow\text{central atom}} + \text{c.n.}_{1\text{·shell}} + \text{c.n.}_{1\text{·}\rightarrow\text{2·shell}} = 1 + 4 + 4 = 9$. [c] Total c.n. = $\text{c.n.}_{2\text{·}\rightarrow\text{1·shell}} + \text{c.n.}_{2\text{·shell}} + \text{c.n.}_{2\text{·}\rightarrow\text{3·shell}} = 1.5 + 3.5 + 2 = 7$. [d] There is no significant bonding between the pairs of Al atoms within the 3rd shell. Only atoms with a distance ranging from 2.5 to 3.0 Å from a particular atom were included and considered for the coordination number.

tion polyhedron can be described as a twice capped distorted pentagonal prism with an idealized 5-fold axis runnig through the Al atoms 4 and 4′. The actual symmetry element is a C_2-axis—parallel to the crystallographic *b*-axis—running through the middle of the Al 6−6′bond, the central Al atom and the center of the plane built up by the Al atoms 2, 3, 2′, and 3′.

The inner shell of **2** can be described as a distorted icosahedron. Due to the fact that the triangles forming the polyhedron are not equilateral, the symmetry is reduced to C_i.

The second shell of **1** (Figure 4a) contains 38 Al atoms. Each of the Al atoms achieves an average coordination number of 7. The polyhedron in this figure is tilted by 90° in comparison to Figure 2.

Characteristic elements of this shell are the exposed Al atoms situated opposite to each other (atoms 14 and 14′). Each of these Al atoms is the intersection point of two triangular and two quadrangular planes. The 2-fold axis points through the quadrangular plane formed by the Al atoms 16, 16′, 17, and 17′ and through the edge between the Al atoms 24 and 24′. Primarily, the shell is formed by an alternating connection of triangles and quadrangles. However, there are also 6 pentagons with larger Al−Al distances (maximum distance 4.863 Å between the Al atoms 16 and 18 in contrast to 4.085 Å between 10 and 12). This connection pattern enables the construction of a shell consisting of only 38 Al atoms around the inner 12-numbered shell.

In **2** (Figure 4b) the situation is different; 44 Al atoms are surrounding the first shell of similar size as in **1**, thus, a different coordination of the atoms should result: the second shell is almost exclusively constructed of triangles and quadrangles. Moreover, four vertexes are pointing to the interior (Al atoms 13, 13′, 21, 21′). The average Al−Al bond lengths are as expected shorter than those in **1** (cf. Tables 3 and 4).

Within the outer shell of **1** and **2** all Al atoms show a 4-fold coordination. However, this is only a topological description. Shell 3 of **1** consists of 18 Al atoms (Figure 5a), the 2-fold axis of symmetry in this representation runs through Al atoms 27 and 28. In **2** (Figure 5b) the ligand-bearing shell is formed by 20 Al atoms.

Table 4. Al−Al Distances within and between (e.g., 1 → 2) the Al_{77} Cluster Shells

shell	center	1	1 → 2	2	2 → 3	3
atoms	1	12		44		20
c.n.	12	9[a]	4	7[b]	2	(4)[c]
$d_{minimal}$ (Å)	2.674	2.693	2.638	2.564	2.565	(4.905)
$d_{maximal}$ (Å)	2.870	2.973	2.991	2.999	2.852	(5.170)
$d_{average}$ (Å)	2.762	2.795	2.818	2.756	2.688	(5.019)

[a] Total c.n. = $c.n._{1\cdot shell\rightarrow central\ atom} + c.n._{1\cdot shell} + c.n._{1\cdot\rightarrow 2\cdot shell} = 1 + 4 + 4 = 9$. [b] Total c.n. = $c.n._{2\cdot\rightarrow 1\cdot shell} + c.n._{2\cdot shell} + c.n._{2\cdot\rightarrow 3\cdot shell} = 1 + 4 + 2 = 7$. [c] There is no significant bonding between the pairs of Al atoms within the 3·shell. Only atoms with a distance ranging from 2.5 to 3.0 Å from a particular atom were included and considered for the coordination number.

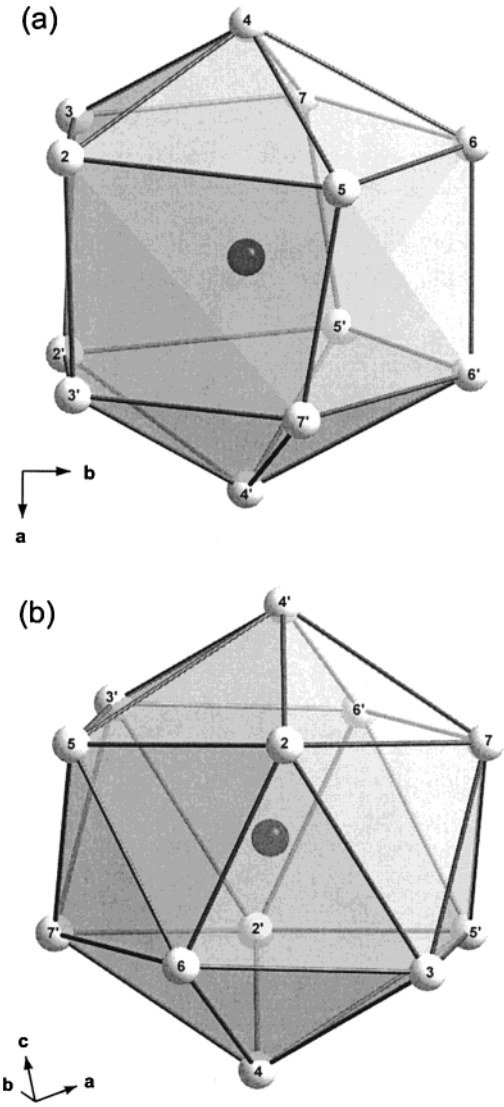

Figure 3. Central Al atom (black) and 1st shell (12 Al atoms) of **1** (a) and **2** (b), each with the same orientation as in the corresponding comprehensive view (**1**, Figure 1; **2**, Figure 2).

In Table 3, the Al−Al distances for **1** within and between the shells are summarized; for comparison the corresponding values of **2** are given in Table 4.

While the average Al−Al distances between the aluminum atoms encapsulated within the 2nd shell (i.e., including the center and the 1st shell) are almost identical in **1**, this does not hold for **2** where the distances slightly increase starting from the center to the second shell. This is surprising considering the more symmetrical arrangement of **2**, where one would rather expect similar bond lengths within the inner shells. Within the

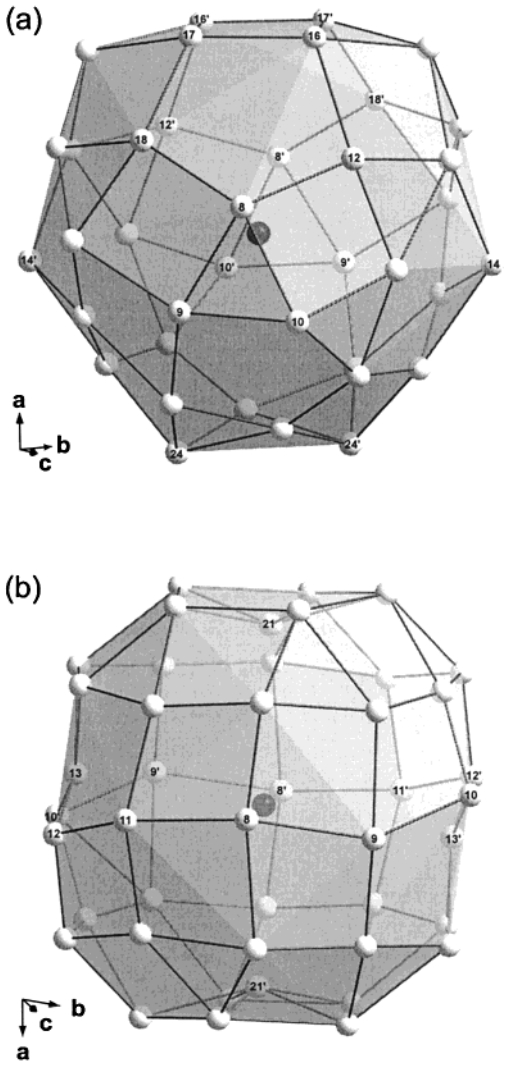

Figure 4. (a) 2nd shell (38 Al atoms) of **1**. (b) 2nd shell (44 Al atoms) of **2** (each central Al atom in black).

second shell, **2** has shorter Al−Al distances than **1**, since in **1** the 12-membered shell is surrounded by only 38 Al atoms, whereas in **2** there are 44 Al atoms which are more densely packed. In both clusters, the shortest bonds are found between the 2nd and 3rd shells. Thus, the bonding relations in the outer sphere are similar to those of subvalent Al compounds with a smaller Al/R ratio,[16] where the average oxidation number of aluminum is closer to +1 (**1**, +0.217; **2**, +0.234).

The arrangement of the shells of **1** and **2** in the space-filling model (Figure 6) shows two significant gaps in the second shell of **1** which allow a closer look on the first shell: In the case of **2** the inner shell is completely covered.

A possible reason for this difference might be the fact that the cavity between the five atoms of the second shell of **1** is larger (distances between opposite Al atoms: 4.807−4.863 Å) than the interstice between the four Al atoms which are covered by an atom of the third shell (3.906−4.009 Å). However, the space-filling cluster model including the $N(SiMe_3)_2$ groups (Figure 7) demonstrates clearly that the cluster core of **1** is almost completely protected by the ligand shell.

(16) Compare the Al−Al bonding lengths (Å) in $[Al_7\{N(SiMe_3)_2\}_6]^-$, 2.540 and 2.737 (ref 11c); $[Al_{12}\{N(SiMe_3)_2\}_8]^{2-}$, 2.542−2.759 (ref 11d); $Al_{12}(AlBr_2\cdot THF)_{10}\cdot 2THF$: 2.526−2.762; reference: Klemp, C.; Köppe, R.; Weckert, E.; Schnöckel, H. *Angew. Chem., Int. Ed.* **1999**, *111*, 1851; *38*, 1739.

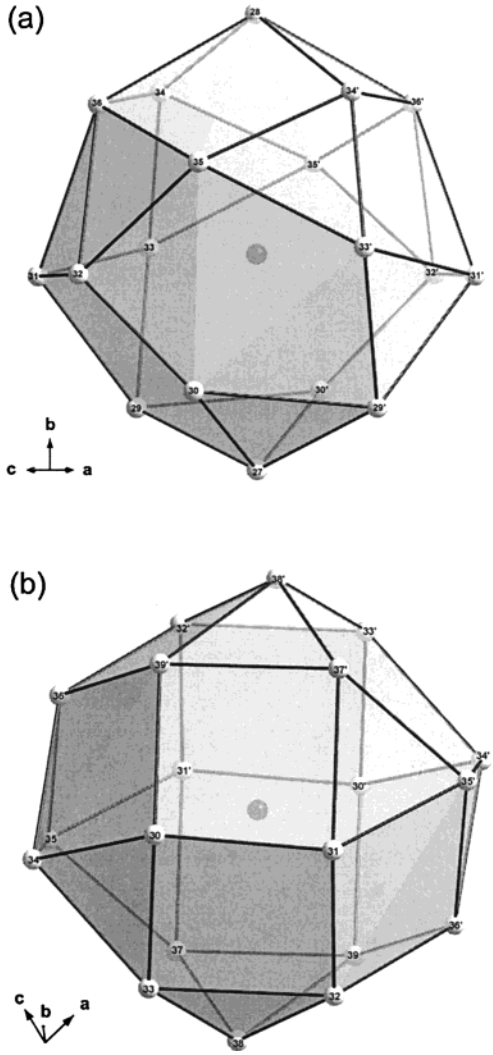

Figure 5. (a) 3rd shell (18 Al atoms) of **1**. (b) 3rd shell (20 Al atoms) of **2** (each central Al atom in black).

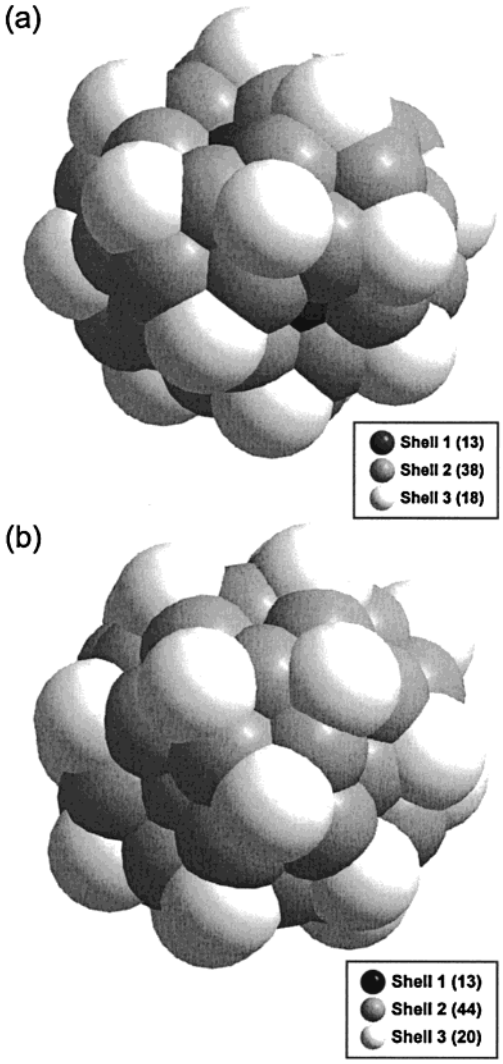

Figure 6. Space-filling model of **1** (a) and **2** (b). Only Al atoms are shown.

Comparison of the Arrangement of Ions in 1a, 1b, and 2 in the Crystal. Figure 8a shows the arrangement of the Al_{69}^{3-} anions, the Li^+ cations, and the solvent molecules in the crystal of **1a**.

The packing of anions reminds of the hexagonal closest packing. Although distortion leads to two longer distances (29.172 Å) within a layer, this description appears to us to be more appropriate than the description as a primitive hexagonal arrangement shown in dashed lines in Figure 8a. In the hexagonal closest packing, the distances of 15.754 Å (31.507/2) between the layers (Figure 8b) are significantly shorter than the distances in the primitive hexagonal arrangement where the shortest distance is 23.820 Å (Figure 8c). In this latter case, however, the layers are displaced distinctly: Therefore the distances from the central Al atom of one layer to the Al atoms of the two vicinal layers vary from 22.669 to 29.172 Å. Turning to the anion closest packing (Figure 8b), the layers are strictly parallel to each other and are placed exactly above each other. In the following, we therefore refer to **1a** as being a distorted hexagonal closest packing.

The "coordination number" between the cluster unit centers can be described as 10+4, because there are 10 shorter distances (av 22.746 Å) and 4 longer ones (av 27.661 Å).

Due to the distortion of the Al_{69}^{3-} anion packing the octahedral interstices are larger and offer sufficient space for two $[Li(OEt_2)_4]^+$ cations. They exhibit an inversion center which lies in the square plane of the octahedron, there is also room for four toluene molecules (Figure 9a). The "tetrahedral" interstices in hexagonal closest packings always appear as pairs of tetrahedra sharing one face to give trigonal bipyramids. A cation is located in the center of each bipyramid; each of the tetrahedral interstices contains a toluene molecule which is not exactly located in the tetrahedron center but skipped to one of

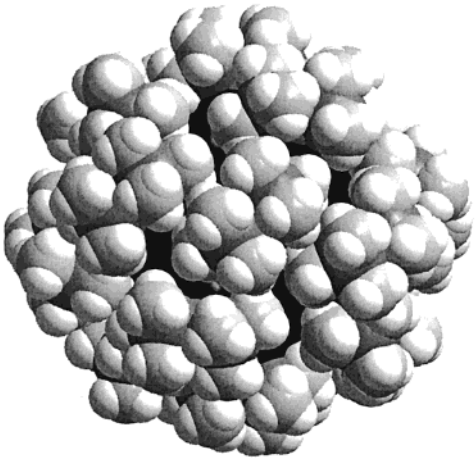

Figure 7. Space-filling model of $[Al_{69}\{N(SiMe_3)_2\}_{18}]^{3-}$.

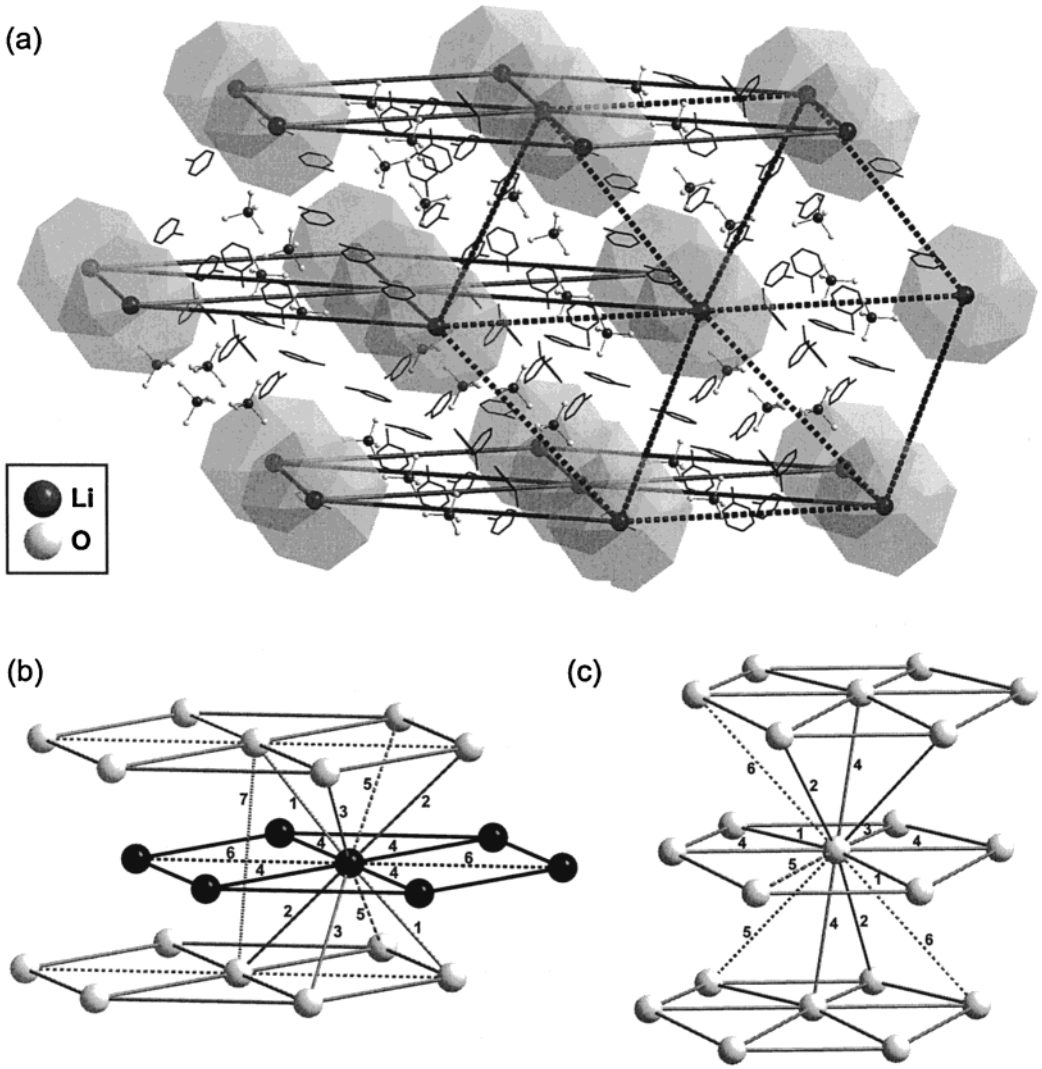

Figure 8. Arrangement of anions (ligands excluded), cations (ethyl groups excluded), and toluene molecules (H atoms excluded) of **1a** in the crystal. (a) View parallel to the layers of the distorted hexagonal closest packing, broken line: coordination of anions within a single layer seen as primitive hexagonal packing. Coordination pattern with hexagonal closest (b) and primitive hexagonal (c) anion packing. Distances (Å): 1, 20.399; 2, 22.669; 3, 23.023; 4, 23.820; 5, 26.149; 6, 29.172; 7, 31.507.

the triangular planes (Figure 9b). The cations in the trigonal bipyramidal interstices are separated by 29.192 and 23.820 Å, corresponding to the parallel connections between the anions. The distances within each cation pair in the octahedral interstices amount to 11.179 Å. With a closest packing having one octahedral and two tetrahedral interstices per packing molecule, **1a** reaches the stoichiometric ratio solvent/cations/anions of 6:3:1. The cations form chains along the stapling direction of the anions (cf. Figure 8a), the distances are identical to those between the anion layers (23.820 Å).

In the primitive hexagonal packing of **2** (Figure 10) the Al_{77}^{2-} anions reach a "coordination number" of 8+4: There are 8 shorter distances (av 22.005 Å) and 4 longer distances (av 27.241 Å). The iodo-bridged Li_2I^+ cations are located in the hexagonal interstices of the anion packing. Additionally, there are two "halves" of toluene molecules per interstice. A comparison of the average distances between the anions to the average distances of **1a** shows that **2** is obviously closer packed (23.750 Å) than **1a** (24.150 Å). The distances within the layers are shorter (**2**, 22.329 Å; **1a**, 25.604 Å), however, in **2** there are longer distances between the layers (**2**, 21.034 Å; **1a**, 15.754 Å). Furthermore, the smaller number of solvent molecules per anion points to a closer packing of **2**. On the other hand, two iodo-bridged $[Li_2I(OEt_2)_5]^+$ cations need more space than three simple $[Li(OEt_2)_4]^+$ cations. Due to the different coordination and charge of the cluster anions in **1a** and **2** a discussion of distances between the cluster anions seems problematic.

The crystal packing of Al_{69} anions in **1b** (Figure 11b) is similar to the arrangement of gallium atoms in β-Ga metal (Figure 11a) with regard to topology and coordination pattern.

The anions in **1b**—like the atoms in β-gallium—form ladders along the *c*-axis and are stapled on top of each other along the *b*-axis in a zigzag pattern. These ladder layers are staggered with respect to the *a*-axis. If we remove the "ladder sides" in a thought experiment, irregular edge-connected hexagons would be present. The cluster anions reach a "coordination number" of 8+6, the shorter distances ranging from 20.273 to 22.736 Å and the longer distances ranging from 27.495 to 28.625 Å; the average value amounts to 24.501 Å (Figure 11c). The cations form chains within canals along the *b*-direction, the distances within the chains being 28.475 Å; between the chains the distances are 18.715 Å. One part of the detected Li^+ cations are positioned in the interstitial lattice sites between the anion "ladder steps", another part of the Li^+ cations—referring to an anion "hexagon" —is located alternatingly on the right and left sides of an anion.[15]

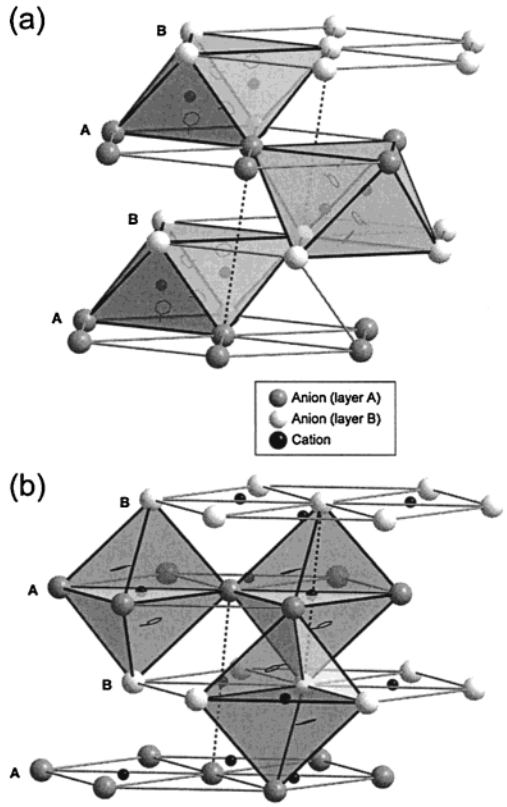

Figure 9. Arrangement of the cations in the octahedral (a) and tetrahedral interstices (b) of the distorted hexagonal closest packing of anions of **1a** in the crystal.

Discussion and Outlook

The differences between **1** and **2** are discussed taking into account the following points: (a) The environment of the central Al atoms, (b) the coordination numbers and distances within the individual shells, and (c) the mechanisms of cluster formation.

(a) One remarkable difference between **1** and **2** arises from the coordination of the central Al atoms. The first shell of **1** displays a distorted decahedral structure (distorted D_{5h} symmetry). However, the respective shell of **2** can be described as icosahedral (distorted cuboctahedron). This difference within the cluster cores is associated with a topologically modified periphery which is shown in the space-filling models in Figure 6. The different arrangements within the cores comes not unexpected, since according to quantum chemical calculations the energetic difference between large, topologically different Al clusters is very small, i.e., approximately ±1% for Al_{55} in various geometries.[17] However, a different topology—as between **1** and **2**—may cause different electronic situations which are more likely to influence the various physical (especially anisotropical) properties. Therefore, an X-ray structural analysis constitutes the only suitable basis for the accurate interpretation of the physical properties. Thus, one has to be cautious when interpreting the physical effects—measured by the usual methods of modern nanotechnology—which are based on the structuring of a surface with an apparently homogeneous cluster species, e.g. the Au_{55} cluster,[18] which has not been characterized by X-ray structural analysis so far.

(17) Binding energy per atom [eV] for a neutral Al_{55} cluster in different symmetries: 2.678 (O_h), 2.652 (I_h). Reference: Ahlrichs, R.; Elliott, S. D. *Phys. Chem. Chem. Phys.* **1999**, *1*, 13.

(18) Schmid, G.; Pfeil, R.; Boese, R.; Bandermann, F.; Meyer, S.; Calis; G. H. M.; van der Velden, J. W. A. *Chem. Ber.* **1981**, *114*, 3634.

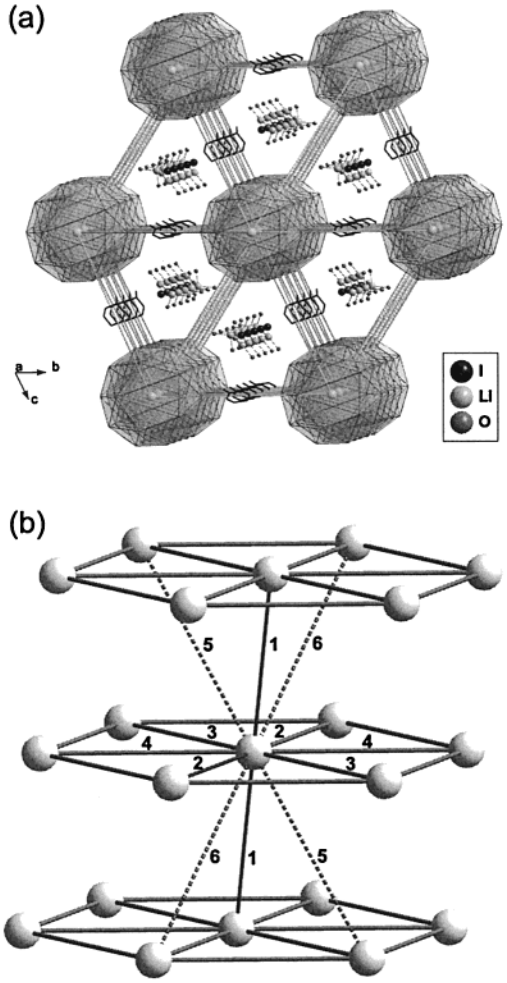

Figure 10. Arrangement of ions of **2** ($N(SiMe_3)_2$ and ethyl groups excluded) within the crystal. (a) View along the stapling direction; (b) coordination pattern with distances (Å) of 1, 21.043; 2, 21.707; 3, 22.154; 4, 23.125; 5, 26.968; 6, 27.514.

(b) In the following, the difference between the 2nd shell (38 and 44 Al atoms) in **1** and **2** will be discussed. According to MACKAY a regular shell built around an icosahedron would lead to a 42-membered shell.[19] This might not be expected for **1** and **2**, since in both cases the inner shell deviates from the icosahedral symmetry. Therefore, our special interest was focused on the volume difference (see below) between the naked clusters Al_{51} (1+12+38 from **1**) and Al_{57} (1+12+44 from **2**), respectively. In Tables 3 and 4 the tendency to decreasing Al−Al bond lengths from the center to the surface becomes evident. The shift of electron density of the Al atoms of the third shell to the nitrogen atoms of the ligands leads to a decrease of the Al−Al bond lengths between these Al atoms and the "naked" Al atoms of the 2nd shell. The electronic influence of the ligands weakens when approaching the cluster center, i.e., the formal oxidation state of the aluminum atoms approaches the value 0 and the distances become more metal-like.[20] However, the arrangement of the "naked" Al atoms in both inner shells differs distinctly from the orientation of the crystalline metal. This can easily be demonstrated by geometrical comparison to a hypothetical Al_{55} fragment from solid cubic face centered aluminum metal (Figure 12).

(19) Mackay, A. L. *Acta Crystallogr.* **1962**, *15*, 916.

(20) The average Al−Al distances between central atom and 1st shell are 2.783 Å (**1**) and 2.762 Å (**2**) and the shortest Al−Al distance in Al metal is 2.855 Å.

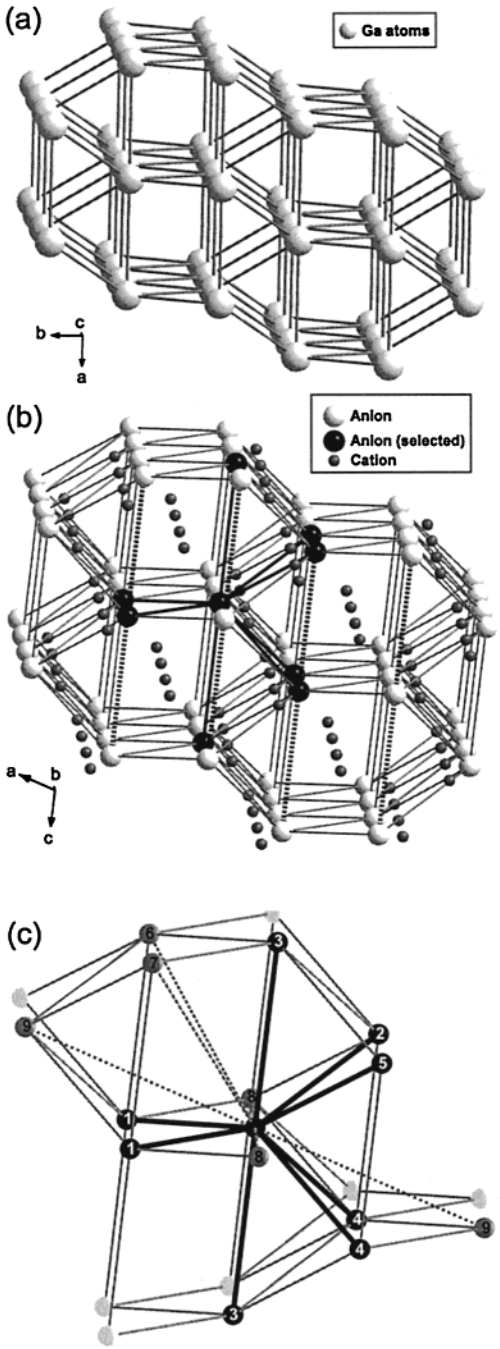

Figure 11. (a) Section of the lattice of metallic β-gallium. Arrangement of ions of **1b** ($N(SiMe_3)_2$, ethyl groups and solvent molecules excluded) within the crystal, view along the crystallographic *b*-axis; (b) the "ladder sides" (cf. text) are marked by dashed lines; (c) coordination pattern in the orientation as in (b) with distances (Å) of 1, 20.273; 2, 21.626; 3, 21.790; 4, 22.226; 5, 22.736; 6, 27.495; 7, 28.376; 8, 28.475; 9, 28.625.

This description sugggests that the Al_{51} (shells 1+2 of **1**) and Al_{57} (shells 1+2 of **2**) cluster cores are more densely packed than in the solid metal.[21] To give a reliable statement about the relative density of Al atoms in the cluster frame, the volumes of the three clusters were calculated each with a charge of −3.[22] As expected, the cluster volume grows with increasing number of atoms, but we can observe a slight decrease in the atomic volume (cluster volume/number of atoms) from Al_{51}^{3-} (29.61 Å) to Al_{57}^{3-} (29.51 Å^3) and Al_{55}^{3-} (29.21 Å^3). Thus, the Al_{55}^{3-} cluster representing a section of the metal has the

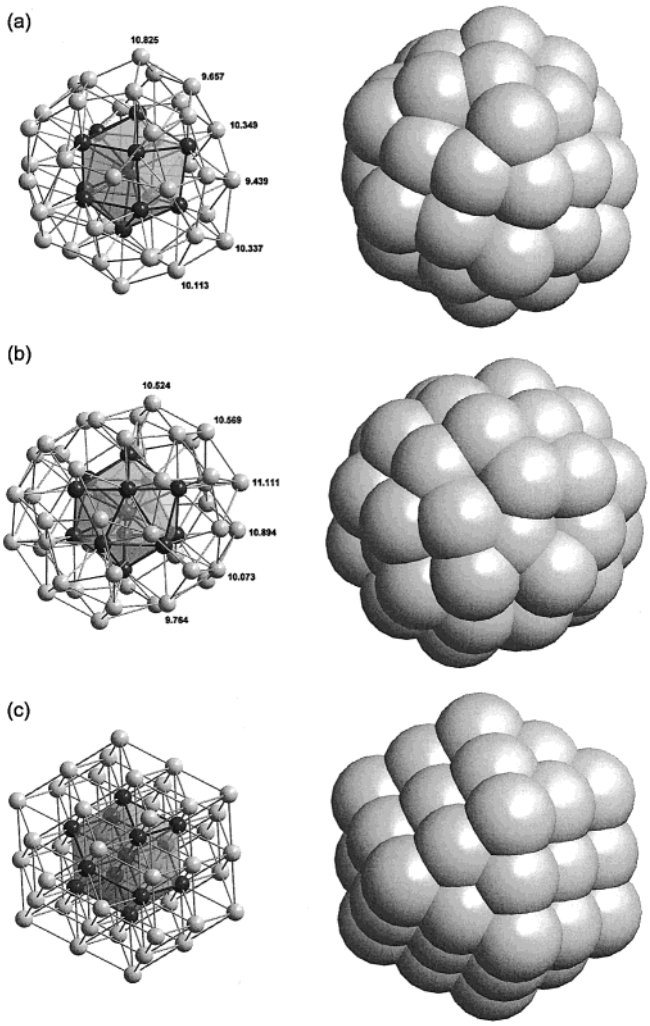

Figure 12. Ball-and-stick models and space-filling models of various Al_n clusters. (a) Shells 1+2 of **1** Al_{51} (1+12+38 atoms). (b) Shells 1+2 of **2**: Al_{57} (1+12+44 atoms). (c) Hypothetical Al_{55} cluster section from the fcc-lattice of Al metal. For Al_{51} and Al_{57} the different diameters are shown in the illustration.

(21) The diameter of constructed Al_{55} (1+12+42 atoms) is 11.42 Å, the average diameter of Al_{51} (1+12+38 atoms) is 10.12 Å and that of Al_{57} (1+12+44 atoms) is 10.47 Å.

(22) To calculate the volume of the clusters we used the experimentally determined coordinates of the naked aluminum cores (−3 charge), i.e., Al_{51}^{3-} (from $[Al_{69}\{N(SiMe_3)_2\}_{18}]^{3-}$), Al_{57}^{3-} (from $[Al_{77}\{N(SiMe_3)_2\}_{20}]^{2-}$) and Al_{55}^{3-} (from the fcc-lattice of Al metal). These coordinates were used as an input for a HF/3-21G* single point calculation (GAUSSIAN98). Using the thereby obtained gas-phase SCF-orbitals the IPCM solvation model (Isodensity Surface Polarized Continuum Model) than constructed an iso(electron)density surface around the Al_n^{3-} ($n = 51, 55, 57$) trianions (isodensity value = 0.0004 e·Å^{-3}). In the output file the within this surface enclosed volume is given. This volume was used for the discussion. References: (a) *IPCM*: Foresman, J. B.; Keith, T. A.; Wiberg, K. B.; Snoonian J.; Frisch, M. J. *J. Phys. Chem.* **1996**, *100*, 16098. (b) *GAUSSIAN98*: Frisch, M. J.; Trucks, G. W.; Schlegel, H. B.; Scuseria, G. E.; Robb, M. A.; Cheeseman, J. R.; Zakrzewski, V. G.; Montgomery, J. A., Jr.; Stratmann, R. E.; Burant, J. C.; Dapprich, S.; Millam, J. M.; Daniels, A. D.; Kudin, K. N.; Strain, M. C.; Farkas, O.; Tomasi, J.; Barone, V.; Cossi, M.; Cammi, R.; Mennucci, B.; Pomelli, C.; Adamo, C.; Clifford, S.; Ochterski, J.; Petersson, G. A.; Ayala, P. Y.; Cui, Q.; Morokuma, K.; Malick, D. K.; Rabuck, A. D.; Raghavachari, K.; Foresman, J. B.; Cioslowski, J.; Ortiz, J. V.; Stefanov, B. B.; Liu, G.; Liashenko, A.; Piskorz, P.; Komaromi, I., Gomperts, R.; Martin, R. L.; Fox, D. J.; Keith, T.; Al-Laham, M. A.; Peng, C. Y.; Nanayakkara, A.; Gonzalez, C.; Challacombe, M.; Gill, P. M. W., Johnson, B.; Chen, W.; Wong, M. W.; Andres, J. L.; Gonzalez, C.; Head-Gordon, M.; Replogle, E. S.; Pople, J. A. *Gaussian 98*, Revision A.3; Gaussian, Inc.: Pittsburgh, PA, 1998.

highest density. In the same order we find an increase of the average coordination number[23] as well as of the average Al−Al distances.[20] According to the pressure-coordination rule and the pressure-distance paradoxon[24] this tendency could be expected: Taking the Al_{51}^{3-} and Al_{57}^{3-} cluster fragments as examples, the transition to metal aluminum can be described as follows: by exerting pressure, the Al atoms in the 2nd shell are squeezed to a smaller volume. This necessarily leads to a simultaneous increase of the coordination number and of the average Al−Al distances. And yet, the density is larger in metallic aluminum as the influence of the higher coordination number overcompensates the interatomic distances.[25] The precipitation of elemental aluminum which we observed in the course of our experiments can be interpreted as the product of a progressing disproportionation of **1** and **2**. During this process the volume of the Al packing changes only slightly, Al atoms must "only" be reorganized which obviously does not require a high activation energy, since the reaction temperature is below 60 °C.

(c) For the stabilization of subvalent aluminum compounds which are synthesized as intermediates during the disproportionation of Al^{I} species—with oxidation numbers between +1 and 0—the $N(SiMe_3)_2$ substituent proved to be very successful. Although five crystalline intermediates with this substituent were characterized so far—$Al_7R_6^-$ (ref 11c), $Al_{12}R_8^-$ (ref 11d), $Al_{14}I_6R_6^{2-}$ (ref 11b), $Al_{69}R_{18}^{3-}$ (**1**), and $Al_{77}R_{20}^{2-}$ (**2**, ref 11a)—more intermediates are required to establish a formation mechanism for **1** and **2**. There is also a fundamental problem: the disproportionation products formed in the system $AlX{\cdot}OEt_2$ (X = Cl, I)/$LiN(SiMe_3)_2$/toluene upon increasing temperature can only be structurally characterized when they crystallize from the solution. Due to the lack of suitable techniques for detection of the dissolved species, only a hypothetical formation mechanism can be formulated, based on the above-mentioned crystal structures and further experimental observations.

During the cluster formation, disproportionation steps ($3\ AlX \rightarrow 2\ Al + AlX_3$)[26] which regulate the growing of the cluster frame as well as metathesis reactions ($AlX + LiR \rightarrow AlR + LiX$),[27] which are responsible for the structure of the ligand shell, have to occur. The growth of the Al_nR_m species (with $n > m$), for instance, could probably proceed by inserting "AlX" units into existing Al−Al bonds with simultaneous separation of AlX_3 species.[28] Once the ligand shell is completed, the cluster core is completely protected, and, therefore, any further reaction by inserting AlX units is impossible.

This hypothetical mechanism of growth, however, provides no clue to the question, why the $N(SiMe_3)_2$ substituent will react to **1** if an AlCl solution is used, whereas **2** is obtained with an AlI solution. A close look at the arrangement of ions within the crystals of **1** and **2** shows that **2** only crystallizes if iodobridged Li_2I^+ cations are offered to the cluster anions, as these cations fit best into the interstices of the primitive hexagonal packing of the $Al_{77}R_{20}^{2-}$ anions. In this case, iodide is required as an halide in order to enable an arrangement of ions within the Al_{77} cluster compound that is favorable for crystal formation. Should **1** and **2** be formed in a similar pathway, it appears possible that the disproportionation process from "AlI" and "AlCl", respectively, to Al metal (and Al^{III} species) would initially lead to the compound with the highest average oxidation number in aluminum, i.e., the $Al_{77}R_{20}^{2-}$ cluster (**2**, +0.234) which will crystallize under the appropriate conditions, e.g., Li_2I^+ as countercation, temperature, and concentration of the solution. With an AlCl solution the system does not fall into the energy mould of **2**, but the reaction will proceed until the $Al_{69}R_{18}^{3-}$ cluster (average oxidation number of Al atoms in **1**: +0.217) is formed, which provides "suitable" cations for crystal formation.

Conclusion

Due to its similarity to the Al_{77} cluster which for the first time was synthesized four years ago, the isolation of an Al_{69} cluster provides the opportunity of a comparison between two of the largest *metalloid* clusters[29] regarding to their chemical structures: both clusters give single crystals which can be structurally characterized by X-ray diffraction. Although similar to a large extent, both clusters demonstrate significant differences in their topologies as well as in their bonding relations which would not have been detected by using the common physical methods of nanotechnology. Nevertheless, the structural results are not sufficient to answer questions pertaining the circumstances which are crucial for the formation of either **1** or **2**, and also to their formation mechanism. For this purpose, further intermediates synthesized on the way from Al^{I} species to Al metal under determined conditions have to be structurally characterized and be discussed also in regard to their formation process.

Acknowledgment. We especially thank F. Neikes and Dr. A. Kornath, working group of Prof. Dr. R. Minkwitz, Institute of Inorganic Chemistry, University of Dortmund, for the special efforts they undertook to investigate the extremely sensitive single crystals by X-ray diffraction measurements. We thank Dr. B. Pilawa, Institute of Physics, University of Karlsruhe, for performing the ESR measurements. Furthermore we thank Dr. H.-J. Himmel for helpful discussions. We are grateful to the Deutsche Forschungsgemeinschaft and the Fonds der Chemichen Industrie for financial support.

Supporting Information Available: An X-ray crystallographic file in CIF format for the structure of $[Al_{69}\{N(SiMe_3)_2\}_{18}][Li(OEt_2)_4]_3{\cdot}6$ toluene (**1a**) and $[Al_{69}\{N(SiMe_3)_2\}_{18}][Li(OEt_2)_3]_2[Li(OEt_2)_4]{\cdot}n$ toluene (**1b**). This material is available free of charge via the Internet at http://pubs.acs.org.

IC0104297

(23) Coordination number in the 2nd shell of **1** and **2**, 7; coordination number in Al metal, 12.

(24) Müller, U. *Anorganische Strukturchemie*; B. G. Teubner: Stuttgart, 1992; p 135.

(25) In an analogous way, an expansion of a metallic Al lattice should lead to a new Al modification with smaller coordination numbers, but also with shorter Al−Al distances and all in all with a larger atomic volume. Reference: $Al_{12}(AlCl_2)_{10}{\cdot}12D$ (*D* = THF, THP): Klemp, C.; Bruns, M.; Gauss, J.; Häussermann, U.; Jansen, M.; Stösser, G.; van Wüllen, L.; Schnöckel, H. *J. Am. Chem. Soc.*, accepted for publication.

(26) A significant difference between either AlX solution applied consists of solvated AlCl being less kinetically stable compared to AlI concerning the disproportionation reaction which finally ends up with the formation of Al metal and the AlX_3.

(27) With AlCl, the metathesis reaction will also proceed faster than with AlI. Therefore—and also due to the lesser disproportionation stability—from AlCl solution the intermediates $Al_7R_6^-$ (ref 11c) and $Al_{12}R_8^-$ (ref 11d) are obtained already at $T < 0$ °C whereas AlI solution only reacts at $T > 50$ °C to $Al_{14}I_6R_6^{2-}$ (ref 11b).

(28) In the course of synthesis of this type the average oxidation numbers within the cluster lattice increase and decrease with each individual step until reaching a final value of 0, i.e., for metal and trihalide, respectively.

(29) With respect to the total number of naked, nonligand-bearing atoms, compound **1** with 51 Al atoms is comparable with **2** (57 Al atoms, ref 11a), the Pd_{145} species (55 Pd atoms, ref 7f), or the Ga_{84} species containing 64 naked Ga atoms (ref 10).